

# Revisiting Weak Energy Condition and wormholes in Brans-Dicke gravity

Hoang Ky Nguyen\*

Department of Physics, Babeş-Bolyai University, Cluj-Napoca 400084, Romania

Mustapha Azreg-Aïnou†

Başkent University, Engineering Faculty, Bağlica Campus, 06790-Ankara, Turkey

(Dated: September 1, 2024)

It is known that the formation of a wormhole typically involves a violation of the Weak Energy Condition (WEC), but the reverse is not necessarily true. In the context of Brans-Dicke gravity, the *generalized* Campanelli-Lousto solution, which we shall unveil in this paper, demonstrates a WEC violation that coincides with the appearance of *unbounded* sheets of spacetime within the region where  $0 < r < r_s$ . The emergence of a wormhole in the region where  $r > r_s$  is thus only an indirect consequence of the WEC violation. Whereas the two regions,  $0 < r < r_s$  and  $r > r_s$ , in general are disconnected by *physical* singularities at  $r = r_s$ , they are both part of the same *mathematical* solution, and their behavior can provide insights into the WEC, which is a *mathematical* property of the solution. Furthermore, we utilize the generalized Campanelli-Lousto solution to construct a Kruskal-Szekeres diagram, which exhibits a “gulf” sandwiched between the four quadrants in the diagram, a novel feature in Brans-Dicke gravity. Overall, our findings shed new light onto a complex interplay between the WEC and wormholes in the Brans-Dicke theory.

## I. INTRODUCTION

Wormholes are hypothetical spacetime structures that may interact with ordinary matter and thus can be observed and even distinguished from black holes [1–15].

To maintain a wormhole, it is often required to violate the Weak Energy Condition (WEC) [16–20]. In its geometric form, the WEC requires that for every future-pointing timelike vector  $t^\mu$ , the inequality

$$G_{\mu\nu} t^\mu t^\nu \geq 0, \quad (1)$$

must hold, where  $G_{\mu\nu}$  denotes the Einstein tensor. Specifically, for the vector  $t^\mu = (1, 0, 0, 0)$ , the WEC yields  $G_{00} \geq 0$ , meaning positive energy density everywhere in any frame of reference. In general relativity (GR), maintaining a wormhole requires the presence of exotic matter, which possesses negative energy density to violate the WEC. However, in generalized or modified theories of GR, the WEC can be violated through the introduction of additional terms or corrections in the gravitational sector. These modifications can effectively simulate the presence of exotic matter without being genuinely exotic. In these scenarios, the *vacuum* field equation involving the metric  $g_{\mu\nu}$  becomes more complex. Nonetheless, it can often be rearranged into the form  $G_{\mu\nu} = \frac{8\pi G}{c^4} T_{\mu\nu(\text{eff})}$  where  $T_{\mu\nu(\text{eff})}$  includes the corrections to the gravitational sector and it acts as a ‘surrogate’ or ‘effective’ source of exotic matter (SET), enabling the violation of the WEC which takes the form,

$$T_{\mu\nu(\text{eff})} t^\mu t^\nu = \frac{c^4}{8\pi G} G_{\mu\nu} t^\mu t^\nu \geq 0, \quad (2)$$

and maintaining wormholes for modified gravity. We emphasize that we are considering Einstein theory of gravity as a reference theory and that the violation of the WEC is regarded with respect to his theory when all extra geometric terms are grouped into an effective SET.

An example of a theory that supports a wormhole is the Brans-Dicke (BD) action. In [21] Agnese and La Camera (ALC) used the Campanelli-Lousto (CL) vacuum solution [22] to show that the BD theory produces a wormhole when the post-Newtonian parameter  $\gamma > 1$  and a naked singularity when  $\gamma < 1$ . They also found that the combination  $(1 - \gamma)(1 + 2\gamma)/(1 + \gamma)$  determines the sign of  $G_{00}$ . While the WEC is indeed violated when a wormhole is formed ( $\gamma > 1$ ), the reverse is not necessarily true, as a violation can also occur when  $-1 < \gamma < -1/2$ , in which case no wormhole is formed.

In this paper, we revisit the analysis of ALC and delve further into the WEC in the BD theory, aiming to answer the question of what happens to spacetime *in the absence of a wormhole* when the WEC is violated. Our findings for BD gravity may have broader implications for modified gravity theories at large [23–29].

The paper is structured as follows. Section II reviews and *generalizes* the existing CL solution so that it is also valid for the region where  $0 < r < r_s$ . This section also analyzes the singularities of the *generalized* CL solution. Section III examines a particular situation in which the solution allows for wormholes. Section IV explores the violation of the WEC. Section V relates the *special* Buchdahl-inspired metric uncovered and examined in Refs. [30, 31, 33, 34] with the *generalized* CL metric. Section VI constructs a Kruskal-Szekeres (KS) diagram for the latter metric. Appendix A gives a brief overview of the Brans solutions, while Appendix B validates the *generalized* CL solution via direct inspection.

\* hoang.nguyen@ubbcluj.ro

† azreg@baskent.edu.tr

## II. EXTENSION OF THE CAMPANELLI-LOUSTO SOLUTION

We shall consider the original BD action [35]

$$\mathcal{S} = \int d^4x \sqrt{-g} \left[ \phi \mathcal{R} - \frac{\omega}{\phi} g^{\mu\nu} \partial_\mu \phi \partial_\nu \phi \right] \quad (3)$$

where  $\phi$  is the BD scalar field and  $\omega$  is the dimensionless BD parameter. Its field equations are given by

$$G_{\mu\nu} = \frac{1}{\phi} (\nabla_\mu \nabla_\nu \phi - g_{\mu\nu} \square \phi) + \frac{\omega}{\phi^2} \left( \nabla_\mu \phi \nabla_\nu \phi - \frac{1}{2} g_{\mu\nu} (\nabla \phi)^2 \right), \quad (4)$$

$$(2\omega + 3) \square \phi = 0.$$

where  $G_{\mu\nu} = \mathcal{R}_{\mu\nu} - g_{\mu\nu} \mathcal{R}/2$  is the Einstein tensor and  $\mathcal{R}$  is the Ricci scalar

$$\mathcal{R} = \frac{\omega}{\phi^2} (\nabla \phi)^2. \quad (5)$$

Brans discovered four solutions in [36], which are expressed in isotropic coordinates and named type I, II, III, and IV, respectively. Among these solutions, the Brans type I solution has been the most explored one, with the other three solutions being “derivable” from it via duality or by taking a proper limit, as we shall discuss in Appendix A. In what follows, we adopt the notation in ALC [21], who were the first researchers to correctly expose the wormhole and naked singularity from the CL solution<sup>1</sup>, which is in essence the Brans type I solution expressed in a different coordinate system [22, 37].

The Brans type I solution comprises of a static spherisymmetric vacuum metric<sup>2</sup>

$$ds_{\text{Brans-I}}^2 = - \left| \frac{1 - \frac{r_s}{4\bar{r}}}{1 + \frac{r_s}{4\bar{r}}} \right|^{2A} dt^2 + \left( 1 - \frac{r_s^2}{16\bar{r}^2} \right)^2 \left| \frac{1 - \frac{r_s}{4\bar{r}}}{1 + \frac{r_s}{4\bar{r}}} \right|^{2B} (d\bar{r}^2 + \bar{r}^2 d\Omega^2) \quad (6)$$

and a scalar field

$$\phi_{\text{Brans-I}} = \phi_0 \left| \frac{1 - \frac{r_s}{4\bar{r}}}{1 + \frac{r_s}{4\bar{r}}} \right|^{-(A+B)} \quad (7)$$

with  $\bar{r}$  being the isotropic radial coordinate. In terms of  $A$  and  $B$ , the BD coupling parameter is

$$\omega = -2 \frac{A^2 + AB + B^2 - 1}{(A + B)^2}. \quad (8)$$

Since  $\omega$  is a parameter of the action, the Brans type I solution effectively involves three parameters,  $r_s$ ,  $\phi_0$  and either  $A$  or  $B$  [related by  $\omega$  (8)]. The Ricci scalar is

$$\mathcal{R} = -(A^2 + AB + B^2 - 1) \frac{128 r_s^{-2}}{\left( \frac{4\bar{r}}{r_s} - \frac{r_s}{4\bar{r}} \right)^4} \left| \frac{1 - \frac{r_s}{4\bar{r}}}{1 + \frac{r_s}{4\bar{r}}} \right|^{-2B}. \quad (9)$$

Note that at the specific point  $\{A = 1, B = -1\}$ , the metric described by (6) simplifies to the Schwarzschild metric expressed in the isotropic coordinate system and the scalar field in (7) reduces to a constant value.

A slightly more illuminating expression can be obtained by “diagonalizing”  $A$  and  $B$ , namely

$$A_{\pm} := \frac{1}{2}(A \pm B). \quad (10)$$

In this notation, the solution is given by

$$ds_{\text{Brans-I}}^2 = \left| \frac{1 - \frac{r_s}{4\bar{r}}}{1 + \frac{r_s}{4\bar{r}}} \right|^{2A_+} \left\{ - \left| \frac{1 - \frac{r_s}{4\bar{r}}}{1 + \frac{r_s}{4\bar{r}}} \right|^{2A_-} dt^2 + \left( 1 - \frac{r_s^2}{16\bar{r}^2} \right)^2 \left| \frac{1 - \frac{r_s}{4\bar{r}}}{1 + \frac{r_s}{4\bar{r}}} \right|^{-2A_-} (d\bar{r}^2 + \bar{r}^2 d\Omega^2) \right\}, \quad (11)$$

$$\phi_{\text{Brans-I}} = \phi_0 \left| \frac{1 - \frac{r_s}{4\bar{r}}}{1 + \frac{r_s}{4\bar{r}}} \right|^{-2A_+}. \quad (12)$$

The conformal factor in the metric is a reciprocal of the scalar field. The proper part of the metric is non-Schwarzschild if  $A_- \neq 1$ . The Ricci scalar is

$$\mathcal{R} = \frac{256 \omega A_+^2 r_s^{-2}}{\left( \frac{4\bar{r}}{r_s} - \frac{r_s}{4\bar{r}} \right)^4} \left| \frac{1 - \frac{r_s}{4\bar{r}}}{1 + \frac{r_s}{4\bar{r}}} \right|^{-2A_+ + 2A_-} \quad (13)$$

The relation (8) is simplified to<sup>3</sup>

$$(2\omega + 3)A_+^2 + A_-^2 = 1. \quad (14)$$

### A. The generalized Campanelli-Lousto solution

From the Brans type I solution, one can obtain the CL solution [22] upon making the coordinate transformation:

$$r = \bar{r} \left( 1 + \frac{r_s}{4\bar{r}} \right)^2 \geq r_s, \quad (15)$$

or, equivalently

$$\left( \frac{1 - \frac{r_s}{4\bar{r}}}{1 + \frac{r_s}{4\bar{r}}} \right)^2 = 1 - \frac{r_s}{r}. \quad (16)$$

For each value of  $r > r_s$  there exist two distinct values  $\bar{r}_1$  and  $\bar{r}_2$  such that  $\frac{4\bar{r}_1}{r_s} = \frac{r_s}{4\bar{r}_2}$ , corresponding to two

<sup>1</sup> Ref. [21] contains several typos. We have identified three sets of misprint. Therein, Eq. (8) should be  $2B + 2$  in place of  $2B$ ; in Eq. (22) all  $-B$  terms should be  $+B$ ; in Eq. (24) the exponent should be  $2(\sqrt{(1+\gamma)/2} - 1)$  instead of  $2(\sqrt{2/(1+\gamma)} - 1)$ .

<sup>2</sup> The Brans type I solution exhibits symmetry upon  $\frac{4\bar{r}}{r_s} \leftrightarrow \frac{r_s}{4\bar{r}}$  producing two symmetric sheets of spacetime across the reflection point  $r_s/4$ .

<sup>3</sup> Note that when the dilation field is a constant, viz.  $A_+ = 0$ , by virtue of (14),  $A_- = \pm 1$  except for  $\omega \rightarrow +\infty$ .

symmetric exterior sheets of spacetime. In the coordinate  $r$ , the Brans type I solution becomes the metric [22]

$$ds^2 = -\left(1 - \frac{r_s}{r}\right)^A dt^2 + \left(1 - \frac{r_s}{r}\right)^B dr^2 + \left(1 - \frac{r_s}{r}\right)^{B+1} r^2 d\Omega^2, \quad (17)$$

and the scalar field

$$\phi(r) = \phi_0 \left(1 - \frac{r_s}{r}\right)^{-\frac{1}{2}(A+B)}, \quad (18)$$

which together comprise the CL solution. It is important to note that the above expressions, as originally reported in [22], are only applicable for the region where  $r > r_s$ . They are not valid if  $A$  or  $B$  takes on a non-integer value. However, it is a straightforward exercise to verify by *direct inspection* that the following *generalized* CL metric and its associated scalar field

$$ds^2 = -\text{sgn}\left(1 - \frac{r_s}{r}\right) \left|1 - \frac{r_s}{r}\right|^A dt^2 + \text{sgn}\left(1 - \frac{r_s}{r}\right) \left|1 - \frac{r_s}{r}\right|^B dr^2 + \left|1 - \frac{r_s}{r}\right|^{B+1} r^2 d\Omega^2, \quad (19)$$

$$\phi(r) = \phi_0 \text{sgn}\left(1 - \frac{r_s}{r}\right) \left|1 - \frac{r_s}{r}\right|^{-\frac{1}{2}(A+B)}, \quad (20)$$

form a solution to the vacuo field equations (4) for all values of  $r \in (0, r_s) \cup (r_s, +\infty)$ , as shown in Appendix B. In the above expressions, the notation “sgn” stands for the signum function. Obviously, the generalized CL solution (19)–(20) reproduces the CL solution (17)–(18) for the region where  $r > r_s$ , but it is also applicable for the region where  $0 < r < r_s$  as well. It also recovers the Schwarzschild metric when  $\{A = 1, B = -1\}$ .

In the *generalized* CL metric,  $g_{tt}$  and  $g_{rr}$  flip their sign across  $r = r_s$  as desired, and the Ricci scalar is

$$\mathcal{R} = -(A^2 + AB + B^2 - 1) \frac{r_s^2}{2r^4} \left|1 - \frac{r_s}{r}\right|^{-B-2} \text{sgn}\left(1 - \frac{r_s}{r}\right). \quad (21)$$

It should be noted that although  $\phi$  remains constant along the line  $A + B = 0$ , the value of  $\omega$  becomes infinite (except at the Schwarzschild point  $\{A = 1, B = -1\}$ ), as deduced from Eqs. (7) and (8). This explains why the metric (6) along the line  $A + B = 0$  can deviate from the Schwarzschild metric.

## B. Singularities

To expose the physical singularities, let us examine the Ricci scalar and the Kretschmann invariant of the generalized CL metric. The Ricci scalar (21) is identically zero on the loci of an ellipse  $A^2 + AB + B^2 = 1$ . See Fig. 1. The Kretschmann invariant is given by [38]

$$\begin{aligned} K &:= \mathcal{R}_{\mu\nu\rho\sigma} \mathcal{R}^{\mu\nu\rho\sigma}, \\ &= 4(\mathcal{R}^{01}_{01})^2 + 8(\mathcal{R}^{02}_{02})^2 + 8(\mathcal{R}^{12}_{12})^2 + 4(\mathcal{R}^{23}_{23})^2, \\ &= \left|1 - \frac{r_s}{r}\right|^{-2(B+2)} \frac{r_s^2}{r^6} \left(6\mathfrak{A} - 2\mathfrak{B} \frac{r_s}{r} + \frac{\mathfrak{C}}{4} \frac{r_s^2}{r^2}\right), \end{aligned} \quad (22)$$

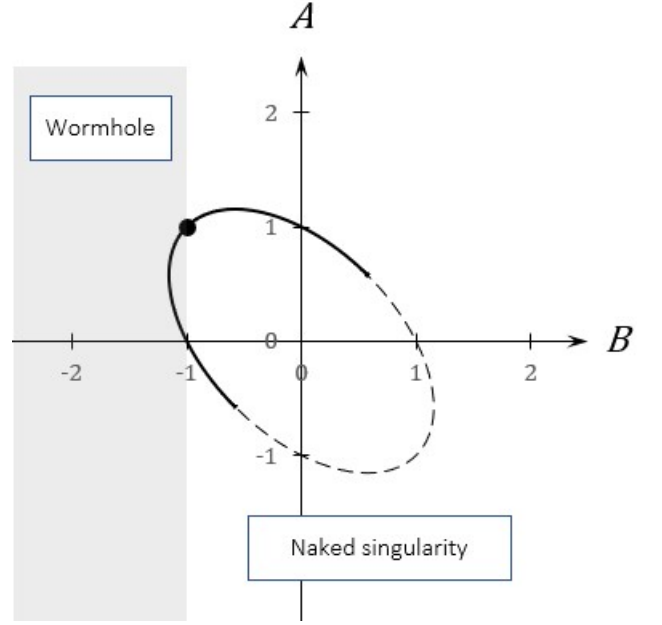


Figure 1. Parameter space of the *generalized* CL metric, Eq. (19). Black dot is Schwarzschild metric  $\{A = 1, B = -1\}$ . The ellipse is the loci  $A^2 + AB + B^2 = 1$  along which the Ricci scalar  $\mathcal{R}$  vanishes for all  $r \in \mathbb{R}$ . The vertical line  $B = -1$  separates the formation of a wormhole (the shaded area) from the naked singularity (the white area). The solid curve segment on the ellipse corresponds to the asymptotically flat Buchdahl-inspired metric, discussed in Sec. V, with the two end points of the segment being  $(1/\sqrt{3}, 1/\sqrt{3})$  and  $(-1/\sqrt{3}, -1/\sqrt{3})$ .

in which

$$\begin{aligned} \mathfrak{A} &= A^2 + B^2, \\ \mathfrak{B} &= A^2(A - 2B + 3) - B(B - 1)(B - 2), \\ \mathfrak{C} &= (A + 1)A^2(A - 2B + 3) \\ &\quad + (3A^2 + B^2 - 2B + 3)(B - 1)^2. \end{aligned} \quad (23)$$

The curvature singularity at  $r = r_s$  exists for  $B > -2$ , except at the two points  $\{A = 1, B = -1\}$  and  $\{A = 0, B = -1\}$ .

While both the the Ricci scalar and the Kretschmann scalar vanish at  $r \rightarrow +\infty$  as  $\mathcal{R} \simeq r^{-4}$  and  $K \simeq r^{-6}$ , they project singularities at  $r \rightarrow 0$  or  $r \rightarrow r_s$ . In these limits, the two scalars show similar behaviors, that is  $K \simeq \mathcal{R}^2$ ,

$$K \simeq \mathcal{R}^2 \simeq \begin{cases} |r - r_s|^{-2(B+2)} & \text{as } r \rightarrow r_s, \\ r^{2(B-2)} & \text{as } r \rightarrow 0, \end{cases} \quad (24)$$

it is thus sufficient to focus on the Kretschmann invariant and the *areal radius*,  $R(r) := r \left|1 - \frac{r_s}{r}\right|^{\frac{1}{2}(B+1)}$ , in our analysis. The summarized results are shown in Table I.

We want to emphasize that the two regions,  $r > r_s$  and  $r < r_s$ , are typically *disconnected* due to the presence of physical singularities located along the separatrix  $r = r_s$ . Generally, there are no geodesics that can traverse from

Case	Range for $B$	$r \rightarrow 0$	$r \rightarrow r_s$	Wormhole or naked singularity ?	Interior region consists of ...	WEC violation ?
[I]	$B \leq -2$	$R$ vanishes $K$ diverges	$R$ diverges $K$ is finite	Wormhole	2 unbounded sheets	Yes
[II]	$-2 < B < -1$	$R$ vanishes $K$ diverges	$R$ diverges $K$ diverges	Wormhole	2 unbounded sheets	Yes
[III]	$-1 \leq B \leq 1$	$R$ is finite $K$ diverges	$R$ is finite $K$ diverges	Naked singularity	4 bounded sheets	No
[IV]	$1 < B < 2$	$R$ diverges $K$ diverges	$R$ vanishes $K$ diverges	Naked singularity	2 unbounded sheets	Yes
[V]	$2 \leq B$	$R$ diverges $K$ is finite	$R$ vanishes $K$ diverges	Naked singularity	2 unbounded sheets	Yes

Table I. Behavior of the areal radius  $R$  and the Kretschmann scalar  $K$  as  $r$  approaches 0 or  $r_s$ . A wormhole is formed when  $R$  exhibits a minimum in the region where  $r > r_s$ . The Weak Energy Condition (WEC) is violated if  $G_{00} < 0$ , see Section IV.

the region where  $r > r_s$  to the region where  $r < r_s$ . However, despite their *physical* disconnection, these regions are part of the same *mathematical* solution, and their behavior can provide insights into the violation of the WEC, which is a *mathematical* property of the solution. Table I also includes the WEC status for completeness, and an elaboration on this topic will be presented in Section IV.

### III. THE CASE OF $B < -1$ : WORMHOLES IN BRANS-DICKE GRAVITY

This section revisits the analysis carried out by Agnese and La Camera [21]. The new element is the behavior of the areal radius  $R(r)$ , produced in Fig. 2.

#### A. Casting in the Morris-Thorne ansatz

In this section, we shall bring metric (19) to the Morris-Thorne ansatz [17]

$$ds^2 = -e^{2\Phi(R)} dt^2 + \frac{dR^2}{1 - \frac{b(R)}{R}} + R^2 d\Omega^2. \quad (25)$$

As a function of  $r$ , the areal radius and its asymptotic behaviors are

$$R(r) = r \left| 1 - \frac{r_s}{r} \right|^{\frac{B+1}{2}} \simeq \begin{cases} r & \text{as } r \rightarrow \infty \\ |r - r_s|^{\frac{1+B}{2}} & \text{as } r \rightarrow r_s, \\ r^{\frac{1-B}{2}} & \text{as } r \rightarrow 0 \end{cases} \quad (26)$$

leading to

$$\frac{dR}{dr} = \text{sgn}\left(1 - \frac{r_s}{r}\right) \left| 1 - \frac{r_s}{r} \right|^{\frac{B-1}{2}} \left[ 1 + \frac{B-1}{2} \frac{r_s}{r} \right]. \quad (27)$$

The redshift function  $\Phi(R)$  is defined via

$$e^{2\Phi(R)} = \text{sgn}\left(1 - \frac{r_s}{r}\right) \left| 1 - \frac{r_s}{r} \right|^A, \quad (28)$$

and the shape function  $b(R)$  via

$$1 - \frac{b(R)}{R} = \frac{1}{1 - \frac{r_s}{r}} \left[ 1 + \frac{B-1}{2} \frac{r_s}{r} \right]^2, \quad (29)$$

with  $r$  being implicit function of  $R$  via Eq. (26). The behavior of  $R(r)$  is shown in Fig. 2. In the region where  $r > r_s$ ,  $R(r)$  exhibits a minimum for  $B < -1$  (represented by Panel D in Fig. 2).

We must note in advance that the graphs shown in Fig. 2 are only “half” of the story. There is a maximal analytic extension of the *generalized* CL metric via the KS diagram, to be constructed in Section VI. The KS diagram “doubles” the coverage of the generalized CL solution, in addition to uncovering a “gulf” sandwiched between the four quadrants.

#### B. The four Morris-Thorne constraints

Let us restrict our consideration to the range  $B < -1$ , of which Panel D in Fig. 2 is a representative.

- The areal radius  $R$  diverges at  $r = r_s$  when  $B < -1$ .
- The equation  $\frac{dR}{dr} = 0$  in (27) has a single root

$$r_* = \frac{1-B}{2} r_s > r_s \quad \text{when } B < -1, \quad (30)$$

with  $R$  attaining a *minimum* value

$$R_* = \frac{r_s}{2} \sqrt{B^2 - 1} \left( \frac{B+1}{B-1} \right)^{\frac{B}{2}}. \quad (31)$$

It is straightforward to verify that when  $B < -1$  the four constraints for the metric to possess a wormhole are met [16, 17], as can be seen in Panel D of Fig. 2: (i) The redshift function  $\Phi(R)$  [defined in (28)] is finite everywhere (hence no horizon); (ii) At the throat of the wormhole,  $R_*$  is the minimum value of  $R$  per Eq. (31);

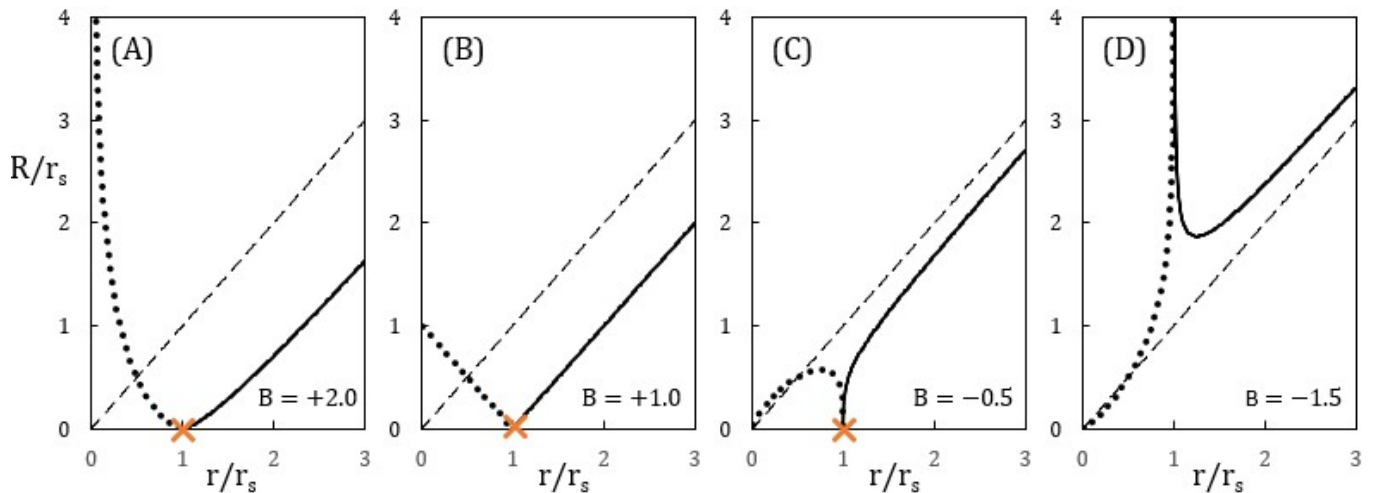


Figure 2. Behavior of the areal radius,  $R/r_s$ , for the *generalized* CL metric versus  $r/r_s$ . Panel D, representative of  $B < -1$ , yields a minimum for  $R(r)$  and corresponds to a wormhole “throat”. Note that the horizon at  $r = r_s$  is non-singular only if  $\{B \leq -2\}$  or  $\{B = -1$  and  $A \in \{0, 1\}\}$ . Some of the plots have been extended to  $r < r_s$  even when the horizon is singular, shown as crosses, with the extension shown in dotted segments. For benchmarking, the dashed lines  $R = r$  are the Schwarzschild metric,  $\{B = -1$  and  $A = 1\}$ .

(iii) The proper radial distance is finite, i.e.  $b(R)/R \leq 1$  for  $R \geq R_*$ . The equality sign holds only at the throat,  $R = R_*$ ; (iv)  $\lim_{R \rightarrow +\infty} [b(R)/R] = 0$  to ensure asymptotic flatness. We emphasize that the throat occurs at location  $r_*$  given in Eq. (30), where the scalars  $\mathcal{R}$  and  $K$  do not diverge (viz. Case I and Case II in Table I), and that, to ensure regularity of the solution everywhere, the lower sheet of the wormhole is a symmetric copy of the existing one (the one corresponding to  $r \geq r_*$ ). The two sheets are *smoothly* glued together at  $r_*$ , ensuring the two-way traversability across the throat from one sheet to the other [34]. The wormhole thus does *not* include the spacetime points where the two scalars diverge.

#### IV. VIOLATION OF THE WEAK ENERGY CONDITION

In its formal geometric form [23], the WEC (2) is violated if the energy density is negative in some region.

The generalized CL metric given in (19) has the 00–component of the Einstein tensor

$$G_{00} = \frac{1 - B^2}{4r^4} r_s^2 \left| 1 - \frac{r_s}{r} \right|^{A-B-2}. \quad (32)$$

Regardless of the value of  $A$ ,  $G_{00} < 0$  when a “throat” is formed, viz. when  $B < -1$ ; see Panel D in Fig. 2. The inequality  $G_{00} < 0$  is interpreted as a signature of negative energy density, resulted from the BD scalar field.

The appearance of a wormhole is associated with a violation of the WEC. However, not all violations of the WEC lead to a wormhole. For example, when  $B > 1$ , the WEC is violated [ $G_{00} < 0 \forall r$  as shown in Eq. (32)], but a wormhole does not appear. This raises the question of what other effects a violation of the WEC can have.

Figure 2 offers an answer to this question. Panels A and D both violate the WEC, but only Panel D exhibits a wormhole, while Panel A does not. However, both panels have something in common: they both feature an unbounded sheet of spacetime in the region where  $0 < r < r_s$  that could exist independently of the region where  $r > r_s$ . In contrast, Panel C has a confined domain consisting of two finite-size “bubbles” glued together<sup>4</sup>. Therefore, a violation of the WEC can alter the topology of spacetime, including that of the region  $0 < r < r_s$ .

For the generalized CL metric, a violation of the WEC leads to a divergence in the cross-section area of the spacetime configuration. This observation might have a broader range of applicability in wormhole physics, beyond Brans-Dicke gravity.

The existence of a wormhole is not a direct consequence of a violation of the WEC, but rather a by-product of a divergence in the areal radius  $R(r)$  at a finite value of  $r$  (whether at  $r = 0$  or  $r = r_s$ ). Thus, a violation of the WEC may or may not result in a wormhole, and only when the divergence of  $R(r)$  occurs at  $r_s$  does a wormhole form.

#### V. MAPPING THE ASYMPTOTICALLY FLAT BUCHDAHL-INSPIRED METRIC INTO THE GENERALIZED CAMPANELLI-LOUSTO METRIC

A particularly interesting case is the loci  $A^2 + AB + B^2 = 1$  in Fig. 1, where  $\omega = 0$  throughout except at

<sup>4</sup> Note that the region where  $0 < r < r_s$  has a mirror image in the KS diagram; see Section VI.

$A = +1, B = -1$ . This loci corresponds to a BD theory with  $\omega = 0$ .

In this section, we aim to establish a connection between the *generalized* CL solution and a vacuum solution that is asymptotically flat at spatial infinity, discovered for pure  $\mathcal{R}^2$  gravity in [30] (see also [31]):

$$ds^2 = |f(r)|^{\tilde{k}} \left[ -f(r)dt^2 + \frac{dr^2}{f(r)} \frac{\rho^4(r)}{r^4} + \rho^2(r)d\Omega^2 \right], \quad (33)$$

with

$$\rho(r) = \zeta r_s \frac{|f(r)|^{\frac{\zeta-1}{2}}}{1 - \text{sgn}(f(r))|f(r)|^\zeta}, \quad (34)$$

$$f(r) := 1 - \frac{r_s}{r}, \quad \zeta := \sqrt{1 + 3\tilde{k}^2}, \quad \tilde{k} := \frac{k}{r_s}, \quad (35)$$

which we named the *special* Buchdahl-inspired metric to reflect its distinctiveness among the class of Buchdahl-inspired metrics. This *special* metric has a vanishing Ricci scalar everywhere,  $\mathcal{R} \equiv 0 \forall r$ , and it is asymptotically flat but not Ricci flat:  $\mathcal{R}_{\mu\nu} \neq 0$  [30]. It is worth mentioning that the discussion made by Higgs [32], following his Eq. (9), concerns only Ricci flat solutions since if  $\lambda = 0$ ,  $R_{\mu\nu} = 0$  too.

To connect the *special* Buchdahl-inspired metric with the *generalized* CL metric, we introduce a new radial coordinate  $r'$  such that

$$1 - \frac{\zeta r_s}{r'} := \text{sgn}\left(1 - \frac{r_s}{r}\right) \left|1 - \frac{r_s}{r}\right|^\zeta \quad (36)$$

The metric presented in (33)–(35) can be transformed into

$$ds^2 = -\left|1 - \frac{\zeta r_s}{r'}\right|^{\frac{\tilde{k}+1}{\zeta}-1} \left(1 - \frac{\zeta r_s}{r'}\right) dt^2 + \left|1 - \frac{\zeta r_s}{r'}\right|^{\frac{\tilde{k}-1}{\zeta}+1} \left[ \frac{dr'^2}{1 - \frac{\zeta r_s}{r'}} + r'^2 d\Omega^2 \right], \quad (37)$$

which is precisely the *generalized* CL metric given by Eq. (19), with an “effective” Schwarzschild radius  $\zeta r_s$ , where

$$A = \frac{\tilde{k} + 1}{\zeta}; \quad B = \frac{\tilde{k} - 1}{\zeta}. \quad (38)$$

It is straightforward to check that the parameters defined in (38) obey the equality (given Eq. 35)

$$A^2 + AB + B^2 = 1 \quad (39)$$

Therefore, the *special* Buchdahl-inspired metric is identical with the *generalized* CL metric with  $\omega = 0$ .

The *special* Buchdahl-inspired metric *simultaneously* belongs to the general Buchdahl-inspired metric family when  $\Lambda = 0$  [30, 31] and to the *generalized* CL solution family when  $\omega = 0$ , representing the intersection of the two families. As such, it is a vacuum solution to two theories at the same time. With  $A$  and  $B$  identified as in (38), the *special* Buchdahl-inspired metric is represented by a solid curve segment in Fig. 2, which corresponds to a portion of the ellipse defined by  $A^2 + AB + B^2 = 1$ .

## VI. CONSTRUCTING KRUSKAL-SZEKERES DIAGRAM FOR THE GENERALIZED CAMPANELLI-LOUSTO METRIC

In our previous work [30], we constructed the KS diagram for the *special* Buchdahl-inspired vacuum solution in pure  $\mathcal{R}^2$  gravity. As demonstrated in the preceding section, this solution has an intimate relationship with the *generalized* CL metric. Therefore, we can adapt the construction method from Ref. [30] to create a KS diagram for the *generalized* CL metric, with suitable adjustments. Figure 3 shows the resulting diagram, which we present in this section.

### A. The Kruskal-Szekeres coordinates

The tortoise coordinate  $r^*(r)$  for the generalized CL metric is defined to satisfy

$$dr^* = \frac{\text{sgn}\left(1 - \frac{r_s}{r}\right)}{\left|1 - \frac{r_s}{r}\right|^{A_-}} dr. \quad (40)$$

The tortoise coordinate (modulo an additive constant) involves a Gaussian hypergeometric function [30]:

$$r^* = \frac{r_s}{1 - A_-} \left|1 - \frac{r_s}{r}\right|^{1-A_-} {}_2F_1\left(2, 1 - A_-; 2 - A_-; 1 - \frac{r_s}{r}\right).$$

Furthermore, by integrating Eq. (40), the difference [if  $A_- \in (-1, 1)$ ]

$$r^*|_{r=0} - r^*|_{r=r_s} = \int_0^{r_s} \frac{dr}{\left(\frac{r_s}{r} - 1\right)^{A_-}} = \frac{\pi A_- r_s}{\sin \pi A_-}. \quad (41)$$

We shall choose the additive constant such that the tortoise coordinate vanishes at  $r = 0$ .

The advanced and retarded Eddington-Finkelstein coordinates are defined as [39, 40]

$$v := t + r^*, \quad u := t - r^*, \quad (42)$$

which, together with (40), give

$$du dv = dt^2 - dr^{*2} = dt^2 - \frac{dr^2}{\left|1 - \frac{r_s}{r}\right|^{2A_-}}. \quad (43)$$

Metric (19) then becomes

$$ds^2 = \left|1 - \frac{r_s}{r}\right|^{A_+} \left\{ -\text{sgn}\left(1 - \frac{r_s}{r}\right) \left|1 - \frac{r_s}{r}\right|^{A_-} du dv + r^2 \left|1 - \frac{r_s}{r}\right|^{-A_+ + 1} d\Omega^2 \right\}. \quad (44)$$

For the KS coordinates [41, 42], we shall consider the two regions  $r > r_s$  and  $r < r_s$  separately.

The  $r > r_s$  region: Let us define

$$X := \frac{1}{2} \left( e^{\frac{v}{2r_s}} + e^{-\frac{u}{2r_s}} \right), \quad T := \frac{1}{2} \left( e^{\frac{v}{2r_s}} - e^{-\frac{u}{2r_s}} \right), \quad (45)$$

giving

$$dT^2 - dX^2 = \frac{e^{\frac{r^*}{r_s}}}{4r_s^2} \left[ dt^2 - \frac{dr^2}{\left| 1 - \frac{r_s}{r} \right|^{2A_-}} \right] = \frac{e^{\frac{r^*}{r_s}}}{4r_s^2} dudv. \quad (46)$$

Metric (44) becomes

$$ds^2 = \left| 1 - \frac{r_s}{r} \right|^{A_+} \times \left\{ -4r_s^2 e^{-\frac{r^*}{r_s}} \left| 1 - \frac{r_s}{r} \right|^{A_-} (dT^2 - dX^2) + r^2 \left| 1 - \frac{r_s}{r} \right|^{-A_-+1} d\Omega^2 \right\}. \quad (47)$$

The  $r < r_s$  region: Let us define

$$X := \frac{1}{2} \left( e^{\frac{v}{2r_s}} - e^{-\frac{u}{2r_s}} \right), \quad T := \frac{1}{2} \left( e^{\frac{v}{2r_s}} + e^{-\frac{u}{2r_s}} \right), \quad (48)$$

giving

$$dT^2 - dX^2 = -\frac{e^{\frac{r^*}{r_s}}}{4r_s^2} \left[ dt^2 - \frac{dr^2}{\left| 1 - \frac{r_s}{r} \right|^{2A_-}} \right] = -\frac{e^{\frac{r^*}{r_s}}}{4r_s^2} dudv. \quad (49)$$

Metric (44) becomes

$$ds^2 = \left| 1 - \frac{r_s}{r} \right|^{A_+} \times \left\{ -4r_s^2 e^{-\frac{r^*}{r_s}} \left| 1 - \frac{r_s}{r} \right|^{A_-} (dT^2 - dX^2) + r^2 \left| 1 - \frac{r_s}{r} \right|^{-A_-+1} d\Omega^2 \right\}. \quad (50)$$

*In combination:* The generalized CL metric in the KS coordinates is thus

$$ds^2 = \left| 1 - \frac{r_s}{r} \right|^{A_+} \times \left\{ -4r_s^2 e^{-\frac{r^*}{r_s}} \left| 1 - \frac{r_s}{r} \right|^{A_-} (dT^2 - dX^2) + r^2 \left| 1 - \frac{r_s}{r} \right|^{-A_-+1} d\Omega^2 \right\}, \quad (51)$$

$$T^2 - X^2 = -\text{sgn} \left( 1 - \frac{r_s}{r} \right) e^{\frac{r^*}{r_s}}, \quad (52)$$

$$\frac{T}{X} = \left( \tanh \frac{t}{2r_s} \right)^{\text{sgn} \left( 1 - \frac{r_s}{r} \right)}. \quad (53)$$

## B. Key aspects of the Kruskal-Szekeres diagram of the generalized Campanelli-Lousto metric

Along the radial direction,  $d\theta = d\phi = 0$ , metric (51) is

$$ds^2 = -4r_s^2 e^{-\frac{r^*}{r_s}} \left| 1 - \frac{r_s}{r} \right|^{A_++A_-} (dT^2 - dX^2). \quad (54)$$

The KS plane for metric (54) (to be called *the CL-KS diagram* hereafter) is illustrated in Fig. 3, which exhibits several significant characteristics:

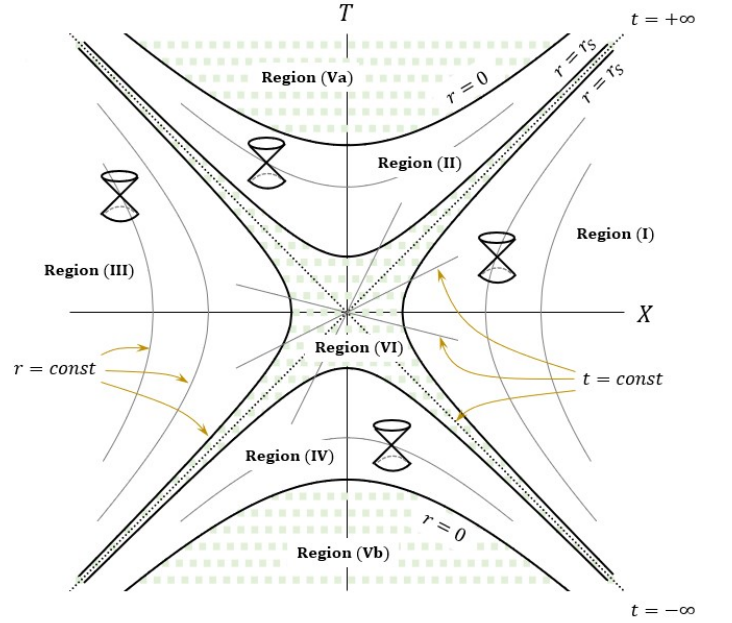


Figure 3. Kruskal-Szekeres diagram for the generalized CL metric when  $A_- \neq 1$ . The “gulf” shown as Region (VI) generally involves curvature singularity at  $r = r_s$ .

- The CL-KS diagram is *conformally Minkowski*. The null geodesics are  $dX = \pm dT$ . Therefore, light cones align along the  $45^\circ$  lines in the CL-KS plane.
- The CL-KS diagram essentially preserves the causal structure of the standard KS diagram, albeit with some quantitative modifications. A constant- $r$  contour corresponds to a hyperbola, while a constant- $t$  contour corresponds to a straight line running through the origin of the  $(T, X)$  plane. The coordinate origin  $r = 0$  amounts to  $T^2 - X^2 = 1$ , since  $r^*(r = 0) = 0$ .
- The separatrix  $r = r_s$  is represented by *two* distinct hyperbolae, per

$$T^2 - X^2 = \begin{cases} -e^{-\frac{\pi A_-}{\sin \pi A_-}} & \text{for } r > r_s \\ +e^{-\frac{\pi A_-}{\sin \pi A_-}} & \text{for } r < r_s \end{cases}. \quad (55)$$

It is worth noting that each hyperbola has two separate branches on its own. For  $A_- = 1$ , the hyperbolae (55) degenerate into two straight lines,  $T = \pm X$ , as is expected for Schwarzschild black holes. In this limit, Region (VI) disappears.

- Region (I) extends up to the right branch of the hyperbola  $T^2 - X^2 = -e^{-\frac{\pi A_-}{\sin \pi A_-}}$ . Region (II) extends up to the upper branch of the hyperbola  $T^2 - X^2 = +e^{-\frac{\pi A_-}{\sin \pi A_-}}$ .
- Regions (III) and (IV) are mirror images of Regions (I) and (II), upon flipping the sign of the KS co-

ordinates, viz.  $(T, X) \leftrightarrow (-T, -X)$ . Regions (Va) and (Vb) are unphysical, viz.  $r < 0$ .

- Region (VI) generally contains the curvature singularity (encoded in the Kretschmann invariant per Eq. (22)) on the separatrix  $r = r_s$ . The region sandwiches between the four hyperbola branches given by (55) and disappears when  $A_- = 1$ .

Further discussions about the causal structure of the  $\zeta$ -KS diagram (for the *special* Buchdahl-inspired metric) have been made in Ref. [30], and we shall not reiterate them here. These discussions are equally applicable for the present case, e.g. the CL-KS diagram, with Region (VI) being a new feature compared with the KS diagram of the Schwarzschild metric.

In summary, the CL-KS diagram represents the maximal analytic extension of the generalized CL metric. The emergence of the ‘‘gulf’’ in the CL-KS diagram indicates fundamental changes in the topology of space-time around a mass source when the metric parameters deviate from their Schwarzschild value, that is when  $(A_+, A_-) \neq (0, 1)$ .

## VII. CONCLUSIONS

Our paper took a crucial step forward by generalizing the CL solution presented in Ref. [22], which was only valid for the region where  $r > r_s$ . Our new *generalized* CL solution holds for all values of the radial coordinate  $r \in \mathbb{R}^+$ , making it applicable to both regions,  $r > r_s$  and  $0 < r < r_s$ . We stress that although in general the two regions are *physically disconnected* by a loci of physical singularities at  $r = r_s$ , they are both part of the same *mathematical* solution. Equipped with this generalization, we are able to revisit and expand upon the analysis previously produced by ALC [21], gaining new insights.

The *generalized* CL metric depends on four parameters: the Schwarzschild radius  $r_s$ , the asymptotic value of the scalar field at spatial infinity  $\phi_0$ , and the exponents  $A$  and  $B$  of the metric components  $g_{tt}$  and  $g_{rr}$ , respectively. The values of  $A$  and  $B$  are related by the BD parameter  $\omega$ . By examining the metric on a two-dimensional plane  $(A, B)$ , we found that for  $B$  in the range  $(-\infty, -1)$ , the metric supports a Morris-Thorne wormhole, while for  $B$  in the range  $(-1, +\infty)$ , a naked singularity results. The value of  $A$  has no effect on this behavior.

We further discovered that violating the WEC does not necessarily lead to the formation of a wormhole. However, it does result in a divergence of the areal radius in the region where  $0 < r < r_s$ , occurring at either  $r = 0$  or  $r = r_s$ . This means that WEC violation causes a change in the topology of spacetime, including in the region where  $0 < r < r_s$ . A wormhole is formed only if the divergence takes place at  $r = r_s$ . Therefore, a wormhole is only an indirect consequence of WEC violation and a by-product of this topology change.

Finally, we established a connection between the *special* Buchdahl-inspired metric, that is known to be asymptotically flat for pure  $\mathcal{R}^2$  gravity [30], and the generalized CL metric. This connection guided us to construct the maximal analytic extension of the generalized CL metric. Figure 3 depicts the KS diagram for this metric, with Region (VI) that sandwiches between the four quadrants representing a new feature for Brans-Dicke gravity.

Overall, our findings indicate a complex interplay between the WEC violation and wormhole formation in Brans-Dicke gravity. The novel features observed in our study provide new insights into the behavior of gravity in this theory, and may have implications for modified theories of gravitation at large.

## ACKNOWLEDGMENTS

We thank the anonymous referees for their valuable feedbacks which helped improve the exposition of this paper. HKN thanks Tiberiu Harko for his helpful insight in conceptualizing this research. We thank Carlos O. Lousto and Valerio Faraoni for their comments, and Valerio Faraoni for pointing out the relevant Refs. [45, 46].

## Appendix A: ON BRANS SOLUTIONS OF TYPE II, III AND IV

Although the relations among the four types of the Brans solutions have been covered in [43–46], we shall reveal one more relation which has been obscure.

The Brans type IV solution can be obtained from the Brans type I solution by sending  $A$  and  $B$  to infinity and  $r_s$  to zero while keeping the products  $A r_s$  and  $B r_s$  fixed. This can be seen as follows. When  $r_s \rightarrow 0$ , the terms  $1 \pm \frac{r_s}{4r}$  are approximately  $e^{\pm \frac{r_s}{4r}}$ ; thus the Brans type I metric (6) and scalar field (7) respectively become

$$ds^2 \approx -e^{-\frac{A r_s}{r}} dt^2 + e^{-\frac{B r_s}{r}} (d\bar{r}^2 + \bar{r}^2 d\Omega^2) \quad (\text{A1})$$

$$\phi \approx \phi_0 e^{\frac{(A+B)r_s}{2r}} \quad (\text{A2})$$

Denote  $B = -(C+1)A$  and  $r'_s = A r_s$ . These expressions yield

$$ds^2_{\text{Brans-IV}} = -e^{-\frac{r'_s}{r}} dt^2 + e^{\frac{(C+1)r'_s}{r}} (d\bar{r}^2 + \bar{r}^2 d\Omega^2) \quad (\text{A3})$$

$$\phi_{\text{Brans-IV}} = \phi_0 e^{-\frac{C r'_s}{2r}} \quad (\text{A4})$$

which form the Brans type IV solution. For a given value of  $\omega \in \mathbb{R}$ , the relation in (8) reads

$$A^2 - (C+1)A^2 + (C+1)^2 A^2 - 1 = -\frac{\omega}{2} C^2 A^2 \quad (\text{A5})$$

With  $A$  being sent to infinity, this relation yields

$$(\omega + 2)C^2 + 2C + 2 = 0 \quad (\text{A6})$$



hence

$$C_{\pm} = \frac{-1 \pm \sqrt{-(2\omega + 3)}}{\omega + 2} \quad (\text{A7})$$

The Brans type III solution is trivially the “mirror” image of Type IV by a reflection,  $\frac{\bar{r}}{r_s} \Leftrightarrow \frac{r_s}{\bar{r}}$ . That is

$$ds_{\text{Brans-III}}^2 = -e^{-\frac{\bar{r}}{r_s}} dt^2 + \frac{r_s^4}{\bar{r}^4} e^{\frac{(C+1)\bar{r}}{r_s}} (d\bar{r}^2 + \bar{r}^2 d\Omega^2) \quad (\text{A8})$$

$$\phi_{\text{Brans-III}} = \phi_0 e^{-\frac{C\bar{r}}{2r_s}} \quad (\text{A9})$$

As was noticed in [43], the Brans type II solution is a curious case. It is a “continuation into the complex plane” by making a formal replacement in the Brans type I solution (6)–(7), per

$$r_s \rightarrow i r_s; \quad A \rightarrow i A; \quad B \rightarrow i B \quad (\text{A10})$$

That is

$$ds_{\text{Brans-II}}^2 = -e^{4A \arctan \frac{r_s}{4\bar{r}}} dt^2 + \left(1 + \frac{r_s^2}{16\bar{r}^2}\right)^2 e^{4B \arctan \frac{r_s}{4\bar{r}}} (d\bar{r}^2 + \bar{r}^2 d\Omega^2) \quad (\text{A11})$$

$$\phi_{\text{Brans-II}} = \phi_0 e^{-2(A+B) \arctan \frac{r_s}{4\bar{r}}} \quad (\text{A12})$$

The relation in (8) becomes

$$\omega_{\text{Brans-II}} = -2 \frac{A^2 + AB + B^2 + 1}{(A+B)^2} \in \mathbb{R}^- \quad (\text{A13})$$

## Appendix B: DIRECT VERIFICATION OF THE GENERALIZED CAMPANELLI-LOUSTO SOLUTION

We directly check that the *generalized* CL metric and scalar field, given in Eqs. (19) and (20), constitute a vacuo solution to the BD field equations. We set  $\nabla_{\mu}\phi\nabla_{\nu}\phi - g_{\mu\nu}\nabla_{\lambda}\phi\nabla^{\lambda}\phi/2 = X_{\mu\nu}$  in BD field equations in vacuo (4). With Eqs. (19) and (20),  $G_{\mu\nu}$  reads

$$\begin{aligned} G_{00} &= \frac{1-B^2}{4r^4} r_s^2 \left|1 - \frac{r_s}{r}\right|^{A-B-2} \\ G_{11} &= \frac{r_s}{4r^4} \frac{(B^2 + 2AB - 2(A+B) + 1)r_s + 4(A+B)r}{\left(1 - \frac{r_s}{r}\right)^2} \\ G_{22} &= \frac{r_s}{4r^2} \frac{(A^2 + A + B - 1)r_s - 2(A+B)r}{1 - \frac{r_s}{r}} \\ G_{33} &= G_{22} \sin^2 \theta. \end{aligned}$$

Next, we have

$$\sqrt{-g} = \left|1 - \frac{r_s}{r}\right|^{\frac{A}{2} + \frac{3B}{2} + 1} r^2 \sin \theta$$

$$\begin{aligned} \sqrt{-g} \square \phi &= \sin \theta \partial_r \left\{ \left|1 - \frac{r_s}{r}\right|^{\frac{A}{2} + \frac{B}{2}} \left(1 - \frac{r_s}{r}\right) r^2 \times \right. \\ &\quad \left. \partial_r \left[ \phi_0 \operatorname{sgn} \left(1 - \frac{r_s}{r}\right) \left|1 - \frac{r_s}{r}\right|^{-\frac{A+B}{2}} \right] \right\} \\ &= 0 \quad \forall r \neq r_s. \end{aligned} \quad (\text{B1})$$

We also have

$$\frac{1}{\phi} \nabla_0 \nabla_0 \phi = \frac{\phi_0 r_s^2}{4r^4} \left|1 - \frac{r_s}{r}\right|^{A-B-2} A(A+B) \quad (\text{B2})$$

$$\begin{aligned} \frac{1}{\phi} \nabla_1 \nabla_1 \phi &= \frac{\phi_0 r_s}{4r^4} \left|1 - \frac{r_s}{r}\right|^{-2} \times \\ &\quad \left[ (2B^2 + 3AB - 2(A+B) + A^2)r_s + 4(A+B)r \right] \end{aligned} \quad (\text{B3})$$

$$\begin{aligned} \frac{1}{\phi} \nabla_2 \nabla_2 \phi &= -\frac{\phi_0 r_s}{4r^2} \left(1 - \frac{r_s}{r}\right)^{-1} \times \\ &\quad \left[ (B^2 + AB - (A+B))r_s + 2(A+B)r \right] \end{aligned} \quad (\text{B4})$$

$$\frac{1}{\phi} \nabla_3 \nabla_3 \phi = \frac{1}{\phi} \nabla_2 \nabla_2 \phi \sin^2 \theta \quad (\text{B5})$$

and

$$X_{00} = \phi_0^2 r_s^2 \frac{(A+B)^2}{8r^4} \left|1 - \frac{r_s}{r}\right|^{-2B-2} \quad (\text{B6})$$

$$X_{11} = \phi_0^2 r_s^2 \frac{(A+B)^2}{8r^4} \left|1 - \frac{r_s}{r}\right|^{-A-B-2} \quad (\text{B7})$$

$$X_{22} = -\phi_0^2 r_s^2 \frac{(A+B)^2}{8r^2 \left(1 - \frac{r_s}{r}\right)} \left|1 - \frac{r_s}{r}\right|^{-A-B} \quad (\text{B8})$$

$$X_{33} = X_{22} \sin^2 \theta \quad (\text{B9})$$

From this stage, it is straightforward to verify, components by components, that the *generalized* CL metric and scalar field in Eqs. (19) and (20) satisfy the BD field equations, viz. Eqs. (4) ( $\square \phi = 0$ ), for all values of  $r \in (0, r_s) \cup (r_s, +\infty)$ .

[1] T. Damour and S.N. Solodukhin, Phys. Rev. D **76**, 024016 (2007), [arXiv:0704.2667](https://arxiv.org/abs/0704.2667) [gr-qc]

[2] C. Bambi, Phys. Rev. D **87**, 107501 (2013), [arXiv:1304.5691](https://arxiv.org/abs/1304.5691) [gr-qc]

- [3] M. Azreg-Ainou, JCAP **07**, 037 (2015), [arXiv:1412.8282 \[gr-qc\]](#)
- [4] V. Dzhunushaliev, V. Folomeev, B. Kleihaus, and J. Kunz, JCAP **08**, 030 (2016), [arXiv:1601.04124 \[gr-qc\]](#)
- [5] V. Cardoso, E. Franzin, and P. Pani, Phys. Rev. Lett. **116**, 171101 (2016), [arXiv:1602.07309 \[gr-qc\]](#)
- [6] R. A. Konoplya and A. Zhidenko, JCAP **12**, 043 (2016), [arXiv:1606.00517 \[gr-qc\]](#)
- [7] K. K. Nandi, R. N. Izmailov, A. A. Yanbekov, and A. A. Shayakhmetov, Phys. Rev. D **95**, 104011 (2017), [arXiv:1611.03479 \[gr-qc\]](#)
- [8] P. Bueno, P. A. Cano, F. Goelen, T. Hertog, and B. Vernocke, Phys. Rev. D **97**, 024040 (2018), [arXiv:1711.00391 \[gr-qc\]](#)
- [9] J. G. Cramer, R. L. Forward, M. S. Morris, M. Visser, G. Benford, and G. A. Landis, Phys. Rev. D **51**, 3117 (1995), [arXiv:astro-ph/9409051](#)
- [10] P. G. Nedkova, V. K. Tinchev, and S. S. Yazadjiev, Phys. Rev. D **88**, 124019 (2013), [arXiv:1307.7647 \[gr-qc\]](#)
- [11] T. Harko, Z. Kovacs, and F. S. N. Lobo, Phys. Rev. D **79**, 064001 (2009), [arXiv:0901.3926 \[gr-qc\]](#)
- [12] E. Deligianni, J. Kunz, P. Nedkova, S. Yazadjiev, and R. Zheleva, Phys. Rev. D **104**, 024048 (2021), [arXiv:2103.13504 \[gr-qc\]](#)
- [13] V. De Falco, M. De Laurentis, and S. Capozziello, Phys. Rev. D **104**, 024053 (2021), [arXiv:2106.12564 \[gr-qc\]](#)
- [14] K. Jusufi, A. Övgün, A. Banerjee, and İ. Sakallı, Eur. Phys. J. Plus **134**, 428 (2019), [arXiv:1802.07680 \[gr-qc\]](#)
- [15] İ. Sakallı and A. Övgün, Astrophys Space Sci **359**, 32 (2015), [arXiv:1506.00599 \[gr-qc\]](#)
- [16] M. S. Morris and K. S. Thorne, Am. J. Phys. **56**, 5 (1988), <https://doi.org/10.1119/1.15620>
- [17] M. S. Morris, K. S. Thorne, and U. Yurtsever, Phys. Rev. Lett. **61**, 1446 (1988), <https://doi.org/10.1103/PhysRevLett.61.1446>
- [18] M. Visser, Nucl. Phys. B **328**, 203 (1989), [arXiv:0809.0927 \[gr-qc\]](#)
- [19] S. Kar, Phys. Rev. D **49**, 862 (1994), <https://doi.org/10.1103/PhysRevD.49.862>
- [20] R. Shaikh and S. Kar, Phys. Rev. D **94**, 024011 (2016), [arXiv:1604.02857 \[gr-qc\]](#)
- [21] A. G. Agnese and M. La Camera, Phys. Rev. D **51**, 2011 (1995), <https://doi.org/10.1103/PhysRevD.51.2011>
- [22] M. Campanelli and C. Lousto, Int. J. Mod. Phys. D **2**, 451 (1993), [arXiv:gr-qc/9301013](#)
- [23] E.-A. Kontou and K. Sanders, Class. Quant. Grav. **37**, 193001 (2020), [arXiv:2003.01815 \[gr-qc\]](#)
- [24] K. K. Nandi and A. Islam, Phys. Rev. D **55**, 2497 (1997) 2497, [arXiv:0906.0436 \[gr-qc\]](#)
- [25] A. G. Agnese and M. La Camera, in Sidharth, B.G., Al-taisky, M.V. (eds) *Frontiers of Fundamental Physics 4*. Springer, Boston, MA, [doi.org/10.1007/978-1-4615-1339-1\\_18](https://doi.org/10.1007/978-1-4615-1339-1_18), [arXiv:astro-ph/0110373](#)
- [26] J. L. Blázquez-Salcedo, C. Knoll, and E. Radu, Phys. Rev. Lett. **126**, 101102 (2021), [arXiv:2010.07317 \[gr-qc\]](#)
- [27] K. Jusufi, S. Kumar, M. Azreg-Ainou, M. Jamil, Q. Wu, and C. Bambi, Eur. Phys. J. C **82**, 633 (2022), [arXiv:2106.08070 \[gr-qc\]](#)
- [28] F. Duplessis and D. A. Easson, Phys. Rev. D **92**, 043516 (2015), [arXiv:1506.00988 \[gr-qc\]](#)
- [29] J. B. Dent, D. A. Easson, T. W. Kephart, and S. C. White, Int. J. Mod. Phys. D **26**, 1750117 (2017), [arXiv:1608.00589 \[gr-qc\]](#)
- [30] H. K. Nguyen, Phys. Rev. D **107**, 104008 (2023), [arXiv:2211.03542 \[gr-qc\]](#)
- [31] H. K. Nguyen, Phys. Rev. D **106**, 104004 (2022), [arXiv:2211.01769 \[gr-qc\]](#)
- [32] P. W. Higgs, Il Nuovo Cimento **11**, 816 (1959), <https://link.springer.com/article/10.1007/BF02732547>
- [33] H. A. Buchdahl, Nuovo Cimento **23**, 141 (1962), [link.springer.com/article/10.1007/BF02733549](https://link.springer.com/article/10.1007/BF02733549)
- [34] H. K. Nguyen and M. Azreg-Ainou, Eur. Phys. J. C **83**, 626 (2023), [arXiv:2305.04321 \[gr-qc\]](#)
- [35] C. H. Brans and R. Dicke, Phys. Rev. **124**, 925 (1961), <https://doi.org/10.1103/PhysRev.124.925>
- [36] C. H. Brans, Phys. Rev. **125**, 2194 (1962), <https://doi.org/10.1103/PhysRev.125.2194>
- [37] L. Vanzo, S. Zerbini, and V. Faraoni, Phys. Rev. D **86**, 084031 (2012), [arXiv:1208.2513 \[gr-qc\]](#)
- [38] K. A. Bronnikov, C. P. Constantinidis, R. L. Evangelista, and J. C. Fabris, [arXiv:gr-qc/9710092](#)
- [39] A. S. Eddington, Nature (London) **113**, 192 (1924), <https://www.nature.com/articles/113192a0>
- [40] D. Finkelstein, Phys. Rev. **110**, 965 (1958), <https://doi.org/10.1103/PhysRev.110.965>
- [41] M. D. Kruskal, Phys. Rev. **119**, 1743 (1960), <https://doi.org/10.1103/PhysRev.119.1743>
- [42] P. Szekeres, Publicationes Mathematicae Debrecen **7**, 285 (1960), <https://inspirehep.net/literature/44776>
- [43] K. Sarkar and A. Bhadra, Class. Quant. Grav. **23** (2006) 6101, [arXiv:gr-qc/0602087 \[gr-qc\]](#)
- [44] V. Faraoni, F. Hammad, and S. D. Belknap-Keet, Phys. Rev. D **94**, 104019 (2016), [arXiv:1609.02783 \[gr-qc\]](#)
- [45] V. Faraoni, F. Hammad, A. M. Cardini, and T. Gobeil, Phys. Rev. D **97**, 084033 (2018), [arXiv:1801.00804 \[gr-qc\]](#)
- [46] K. A. Bronnikov, Acta Phys. Polon. B **4**, 251 (1973), <https://www.actaphys.uj.edu.pl/fulltext?series=Reg&vol=4&page=2>